Phase reconstruction of a strong-laser-field-excited complex molecular system

Yanghua Zhang, Zhenhao Wang, Quanjun Wang, Jingjie Ding, Shaohua Sun, Zuoye Liu,* and Bitao Hu†
School of Nuclear Science and Technology, Lanzhou University, 730000, China

(Received 9 January 2018; revised manuscript received 11 April 2018; published 18 September 2018)

We study the dynamic evolution of the excited dye molecule IR144 in the liquid phase by performing transient-absorption measurement. The time-delay-dependent absorption spectra show different behaviors when the pump pulse either precedes or follows the probe pulse. Assuming the excited molecule as a multilevel system, we reproduce the experimental results based on the density matrix theory. As a system's quantum dynamics is closely related to its absorption spectral shape, the quantum evolution of the excited dye molecule IR144 is analyzed and the system's phase information is extracted from the intensity-dependent absorption spectra. The present work finds us a route for the full understanding and control of the quantum dynamics in a complex system excited by an external pulsed laser field.

DOI: 10.1103/PhysRevA.98.033412

I. INTRODUCTION

Light-matter interaction is a key process in physical systems on any length scale, and one of the most important processes is absorption [1]. With the development of ultrashort laser pulses, transient-absorption spectroscopy (TAS) [2–7] becomes one of the most powerful experimental tools to study the dynamics of a variety of systems in strong fields, e.g., the electronic dynamics in atoms, molecules, and nanoparticles dressed by a strong laser field on its natural timescale [8–15], the excited-state dynamics of atoms and molecules [16–20], laser-induced nuclear dynamics in molecules [21,22], and carrier dynamics in semiconductors [23,24]. Investigations with inverted arrival order of the pump and probe pulses were performed to study the pump-pulse intensity-dependent absorption line shape [25–27], which was understood as the electronic dipole modulation. Another interesting scientific prospect is the reconstruction of coherent electronic wave packets using TAS, with appropriate pulses in the optical or ultraviolet regimes [20,28–31]. TAS includes both amplitude and phase information about an excited quantum system, realizing the reconstruction of the aimed system's wave packet in both space and time.

Bound states play a major role in the quantum dynamics of systems with chemical and biological interest. Femtosecond laser pulses are widely applied to investigate wave-packet dynamics (e.g., dissociation reaction, atom transfer, isomerization) in molecules, resulting in the understanding of chemical bonds and opening the field of femtochemistry [32]. However, the investigations focusing on the dynamic evolution of complex systems excited by strong fields have not successfully studied the detailed phase information of the excited wave packets. Phase defines the shape of a wave packet and hence determines its subsequent time evolution, which is very important for the reconstruction of an excited system. Many techniques were developed to study the phase information of an excited system in both gas and liquid phase, e.g., time resolved coherent Raman scattering [33] and time resolved photoelectron spectroscopy [34]. Among these methods, the two-dimensional (2D) spectroscopy developed from TAS was widely used to study the dynamics of polyatomic molecules in the liquid phase [35,36]. However, to the author's knowledge, 2D spectroscopy has not thus far been used to address the question of phase interruptions in an evolving system by an intense pulse. In very recent work, Meyer *et al.* [37] studied the phase information of an excited bound, molecular wave packet by assuming it to be a multilevel system. However, it was still restricted to the case that the pump pulse follows the probe pulse, and the dynamic process of the case that the pump pulse precedes the probe pulse was ignored.

In this paper we measure the transient-absorption spectra in the dye molecule IR144 based on the pump-probe configuration in Fig. 1(a). Assuming the molecule to be a multilevel system, we analyze the relationship between the dynamic evolution of the excited system and its absorption spectral shape. The phase information is extracted from absorption spectra, when the dynamics are either triggered or modified by the intense pump pulse.

II. THEORETICAL MODEL

A. Multilevel system for IR144

The molecular structure of the dye IR144 is very complex, and its electronic and vibrational energy levels are extremely difficult to estimate. We try to understand it in a simple way. Figure 1(b) shows the molecular structure, and the central chain consists of conjugated double bonds as marked with the green box, resulting in a planar geometry. The sequence of conjugated double bonds with a nitrogen atom on the left and right side provides an extended π-electron system [38]. The π electrons are trapped in this nitrogen-carbon chain, corresponding to the particle-in-a-box principle. The energy levels of a particle-in-a-box are $E_n = \frac{n^2h^2}{8mL^2}$, where m is the electron

*Corresponding author: zyl@lzu.edu.cn
†Corresponding author: hubt@lzu.edu.cn

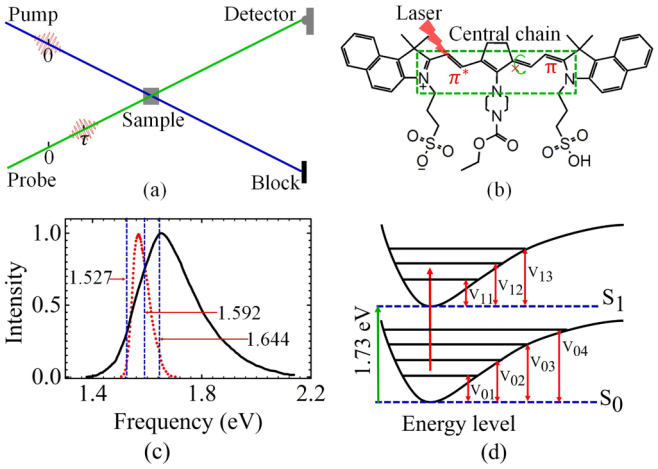

FIG. 1. (a) The transient-absorption measurement schematic based on the pump-probe configuration. The absorption spectrum of the probe pulse are measured with a time delay τ respecting the pump pulse after interacting with the target. The positive time ($\tau > 0$) means the pump pulse precedes the probe pulse. (b) The structure of the dye molecule IR144. (c) The absorption spectrum of the dye molecule IR144 (the black solid line) and the laser spectrum measured before the sample (the red dotted line). (d) The multilevel scheme used to model the dye molecule IR144 interacting with the laser pulses.

mass, L is the box length, n is the orbital quantum number, and h is Planck's constant. These π electrons can move freely along the conjugated chain of the molecule IR144, and the lowest energy electronic transition is the excitation of this π-electron system. When a laser pulse interacts with the target molecule, one π electron will be excited from the highest occupied molecular orbital (HOMO) to the lowest unoccupied molecular orbital (LUMO), i.e., from the ground state to the first excited state. The transition energy can be given as

$$\Delta E = \frac{h^2}{8mL^2}(2n_{\mathrm{HOMO}} + 1). \tag{1}$$

The central chain of IR144 contains five double bonds. There are two π electrons for every double bound, and the lone pair of the nitrogen atom also takes part in the π bonding, hence 12 electrons have to be considered in total. According to Pauli's exclusion principle, each molecular orbital is filled with two π electrons, thus $n_{\mathrm{HOMO}} = 6$. There are 12 bonds in the nitrogen-carbon central chain, the typical length of a conjugated bond is about 0.14 nm, consequently the box length $L = 1.68$ nm. The transition energy of a π electron in IR144 is $\Delta E = 1.73$ eV, which is taken as the theoretical energy difference between the first excited and ground states.

For the complex molecular system, a number of vibrational states superimpose on the main levels. The absorption spectral profile of IR144 can be taken as the collective effect of numbers of different electronic dipole transitions from the vibrational states on the ground state to that on the first excited state. The lifetime of vibrational states on the first excited state is very short due to the intramolecular and intermolecular interactions, resulting in the broad absorption spectrum shown in Fig. 1(c). The vibrational states on the ground and first excited states are calculated by Mewes *et al.* based on density functional theory [39]. They solved the Schrödinger equation for the electrons in the field of the nuclei, using the Born-Oppenheimer approximation. After the electronic wave functions of the ground and excited states are obtained, the frequencies of vibrational states are calculated by the conventional method of diagonalizing the Hessian matrix. The vibration energies on the ground and the first excited state are in the range from 2 to 16 meV. Considering our fundamental purpose is to qualitatively investigate and understand the phase modulation of the IR144 molecular system, a uniform space of vibration transitions 13 meV is selected as the final energy space of vibration transitions. As the spectrum of the laser pulse used in the measurement has a frequency range from 1.512 to 1.685 eV with a center frequency of 1.569 eV, not all of these electronic transitions will be excited during the interaction. For the present case, four vibrational states on the ground state and three on the first excited state with strongest contributions are selected, and ten electronic transitions are employed to model the laser and molecule interaction, as marked in Fig. 1(d). The frequencies of ten transitions are chosen from 1.527 to 1.644 eV.

B. Phase extraction

The schematic for the transient-absorption measurement is shown in Fig. 1(a). The pump and probe pulses are centered at $t = 0$ and $t = \tau$, respectively, i.e., they are delayed with a time τ. The pump pulse precedes the probe pulse for $\tau > 0$ (pump-probe side) and follows it for $\tau < 0$ (probe-pump side). The absorption spectrum of the probe pulse can be measured after interacting with the target. The evolution of a multilevel system can be characterized by the density matrix formulated in the electric dipole approximation. For the single electronic transition between levels $|i\rangle$ and $|j\rangle$ [40], the off-diagonal element denotes the coherence while a diagonal element quantifies the population of level $|i\rangle$.

On the probe-pump side, the probe pulse will come first to interact with the system at $t = \tau$. The electronic transition between levels $|i\rangle$ and $|j\rangle$ will be excited and decay with time-dependent coherence

$$\hat{\rho}_{ij}(t) \propto \frac{i}{\hbar}\left[\int_{-\infty}^{t} dt' e^{-i\omega_{ij}t'} E_{\mathrm{L}}(t')\right] e^{-\frac{\Gamma_{ij}}{2}t} e^{i\omega_{ij}t}. \tag{2}$$

Here ω_{ij} is the frequency for the transition from the level $|i\rangle$ to $|j\rangle$, Γ_{ij} represents the corresponding decay width, and $E_{\mathrm{L}}(t')$ denotes the time-dependent laser electric field. If the intense pump pulse is then applied to interact with the system at $t = 0$, it will cause a shift of the resonance-transition frequency due to the dynamical Stark effect. The modified frequency $\widetilde{\omega}_{ij}(t)$ depends on the pump-pulse intensity [38],

$$\widetilde{\omega}_{ij}(t) = \omega_{ij} + d\omega(t) = \omega_{ij} + C I_{\mathrm{pump}}(t), \tag{3}$$

where C is a coupling coefficient to determine the magnitude of frequency shift caused by the intense pump pulse, $I_{\mathrm{pump}}(t)$ denotes the time evolution of the pump-pulse intensity, and $d\omega(t)$ depends on time during the pump pulse duration. For the single transition $|i\rangle \rightarrow |j\rangle$, the modulation can be simulated by changing the ω_{ij} to be $\widetilde{\omega}_{ij}(t)$ at $t = 0$ in Eq. (2), and

the electronic dipole in the time domain is

$$\hat{\rho}_{ij}(t,\tau) \propto \begin{cases} \frac{i}{\hbar}\Big[\int_{-\infty}^{t} dt' e^{-i\omega_{ij}t'} E_{\mathrm{L}}(t')\Big] e^{-\frac{\Gamma_{ij}}{2}t} e^{i\omega_{ij}t}, & t<0, \\ \frac{i}{\hbar}\Big[\int_{-\infty}^{t} dt' e^{-i\widetilde{\omega}_{ij}(t')t'} E_{\mathrm{L}}(t')\Big] e^{-\frac{\Gamma_{ij}}{2}t} e^{i\widetilde{\omega}_{ij}(t)t}, & t \geqslant 0. \end{cases} \tag{4}$$

In an atomic system, the modulation effect is summarized as the self- and interstate contributions [27,41]. Since ten different transitions are considered for the molecular system, and these vibrational states are close to each other, the interstate contributions are ignored to simplify the model. A phase change ϕ is introduced to the electronic dipole at its arrival time $t = 0$,

$$\phi = \int dt d\omega(t) = C \int dt I_{\mathrm{pump}}(t), \tag{5}$$

which is integrated in the duration of pump pulse, i.e., the modulation can be quantized by the phase change of the electronic dipole. The spectral response of the electronic dipole can be given by Fourier transforms of Eq. (4), and an additional phase change to the dipole results in the modulation of its spectral shape in frequency domain. The repetition period for the phase change is 2π, and one specific spectrum can be generated by only one phase change in a phase cycle [25].

The measurable time-delay-dependent OD absorption spectrum relates to the time evolution of the off-diagonal elements via Fourier transforms at the arrival time of the probe pulse [42]. There is not only one single transition in the dye molecule IR144, but ten possible excitations. The response of the system in time domain can be given as $\sum \hat{\rho}_{ij}(t,\tau)$. The time-delay-dependent spectral response is

$$S_{\mathrm{ab}}(\omega,\tau) \propto \frac{-\mathrm{Im}\big[\sum \int_{-\infty}^{\infty} \rho_{i,j}(t,\tau) e^{-i\omega(t-\tau)} dt\big]}{E_{\mathrm{pr}}(\omega)}, \tag{6}$$

with Fourier transforms centered at the arrival time of the probe pulse $t = \tau$, and $E_{\mathrm{pr}}(\omega)$ denotes the spectrum of the probe pulse before interaction. The time-dependent absorption spectrum of the molecular system can be taken as the accumulation of the spectral responses of these ten different electronic dipoles. Both the pump and probe pulses are described by the classical Gaussian wave packets. The absorption spectrum on the probe-pump side is thus modeled. While on the pump-probe side, the molecular system will be both excited and modulated by the pump pulse. The frequencies of these ten transitions become time dependent right after the excitation, i.e., a phase change to each dipole at $t = 0$. The probe pulse only plays the role to probe the time evolution of the molecular system.

To extract the phase information from the measured absorption spectra, we globally fit the experimental results by the simulation. The excited dipoles evolve freely if the pump-pulse intensity is zero. The absorption spectrum reflects truly the physical information of the excited system, the decay constant is determined to be 0.03 fs^{-1} by fitting the measured absorption spectrum without pump pulse. The phase changes of these ten electronic dipoles are denoted by $\phi_{\mathrm{N},i}$ ($i = 1, 2, 10$) on the probe-pump side. The ten phase changes are first varied in the range from 0 to 2π (one phase cycle) with a step of 0.2π to calculate the simulation results by Eq. (6) to match a given experimental measured spectrum. That is to say 10^{10} sets of phase change $\{\phi_{\mathrm{N},i}\}$ are tried. The residual sum of squares according to the least-square method,

$$\chi^2 = \sum_{\{\phi_{\mathrm{N},i}\}} \Big[S_{\mathrm{ab}}^{\phi_{\mathrm{N},i}}(\omega,\tau) - S_{\mathrm{expt}}(\omega,\tau)\Big]^2 \tag{7}$$

is used to evaluate the set of phase changes $\{\phi_{\mathrm{N},i}\}$ on the probe-pump side, which is also applied in the study of electronic transport characterization of silicon wafers [43]. Here χ^2 is the residual sum of squares, $S_{\mathrm{ab}}^{\phi_{\mathrm{N},i}}(\omega,\tau)$ is the simulated result calculated by Eq. (6) corresponding to one set of phase changes $\{\phi_{\mathrm{N},i}\}$, and $S_{\mathrm{expt}}(\omega,\tau)$ is the experimental result. The minimal residual sum of squares χ^2 corresponds to a set of phase changes $\{\phi_{\mathrm{N},i}^1\}$, which is used as the basis solution. These phase changes are secondly varied in relative ranges of $[\phi_{\mathrm{N},i}^1 + 0.2\pi,\ \phi_{\mathrm{N},i}^1 - 0.2\pi]$ with a step of 0.04π to get another set of phase changes $\{\phi_{\mathrm{N},i}^2\}$ corresponding to the minimal χ^2. Now these phase changes are limited in relative ranges $[\phi_{\mathrm{N},i}^2 + 0.04\pi,\ \phi_{\mathrm{N},i}^2 - 0.04\pi]$. Different from the former two steps, we simultaneous change $\phi_{\mathrm{N},i}$ with a step of $10^{-3}\pi$ to save the time. A set of phase changes $\{\phi_{\mathrm{N},i}^3\}$ is acquired according to Eq. (7), which are then checked manually by comparing the simulation result with the experimental one. If obvious differences are found, the phase change of one electronic dipole is selected randomly in $\{\phi_{\mathrm{N},i}^2\}$ to shift by a step of $10^{-3}\pi$, and these phase changes are simultaneously tuned again with the step of $10^{-3}\pi$ until the simulation absorption spectrum matches the experimental one reasonably well. The final achieved set of phase change $\{\phi_{\mathrm{N},i}^{\mathrm{B}}\}$ will be presented as the extracted phase information on the probe-pump side. The phase changes on the pump-probe side denoted by $\{\phi_{\mathrm{P},i}^{\mathrm{B}}\}$ can be obtained by the same way as that on the probe-pump side.

The residual sum of squares χ^2 as a function of the relative phase changes $\Delta\phi_{\mathrm{N},i}$ are calculated to exam the reliability of the extracted phase information on the probe-pump side by setting $\{\phi_{\mathrm{N},i}^{\mathrm{B}}\}$ as the relative origin of coordinates, i.e., $\phi_{\mathrm{N},i}$ ($\phi_{\mathrm{P},i}$) are simultaneously changed respecting $\{\phi_{\mathrm{N},i}^{\mathrm{B}}\}$ in a relative range of $\pm 0.6\pi$. Figure 2(a) shows these results obtained when the pump-pulse intensities are 1.2×10^{10}, 3.6×10^{10}, 5.4×10^{10}, 7.2×10^{10}, and 9.0×10^{10} $\mathrm{W/cm^2}$. The residual sum of squares χ^2 with varying relative phase changes $\Delta\phi_{\mathrm{P},i}$ on the pump-probe side are also calculated and displayed in Fig. 2(b). It can be found that the minimal χ^2 for all these pump-pulse intensities are located around $\Delta\phi_{\mathrm{N},i} = 0$ on the probe-pump side and $\Delta\phi_{\mathrm{P},i} = 0$ on the pump-probe side, demonstrating that the phase extraction method is reliable within the margin of error. The modulation effect due to the intense laser field shown by the absorption spectrum can be quantified by the extracted phase information.

III. EXPERIMENTAL SETUP

The experimental setup for the transient-absorption measurement of IR144 are shown in Fig. 3. A Ti:sapphire femtosecond laser system is employed, which supplies pulsed laser with a central frequency of 1.569 eV, maximum pulse

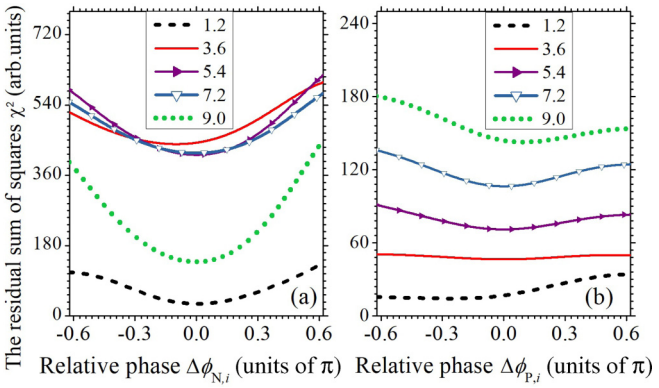

FIG. 2. The dependence of the residual sum of squares χ^2 on the relative phase changes on (a) the probe-pump and (b) pump-probe sides, respectively. Different lines in each panel correspond to different pump-pulse intensities. The coordinates of x axis is just a relative location respecting these phase changes $\{\phi^{B}_{N,i}\}$ or $\{\phi^{B}_{P,i}\}$.

energy of 1.2 mJ, repetition rate of 1 kHz, and pulse duration of 35 fs. In the traditional configuration of the transient-absorption measurement, the probe and pump beams are both focused to interact with the target sample in order to increase the power density. For our case, high power density is not necessary but the size of interaction area is. A telescope is set into the beam path right after the laser system to shrink the laser beam in diameter (5:1), satisfying both the requirement of the laser power density and the size of the interaction area. Afterwards, the laser beam is split into two arms, serving as the pump and probe beams, which propagate independently along a respective optical path. The intensities of the probe and pump pulses can be changed by the continuously neutral-density (ND) filters Fl and F2, respectively. A delay line constituted by two high reflectivity mirrors M1, M2 and a stage (Zolix, TSA50-C) is included into the pump beam path to change the time delay τ between the pump and probe

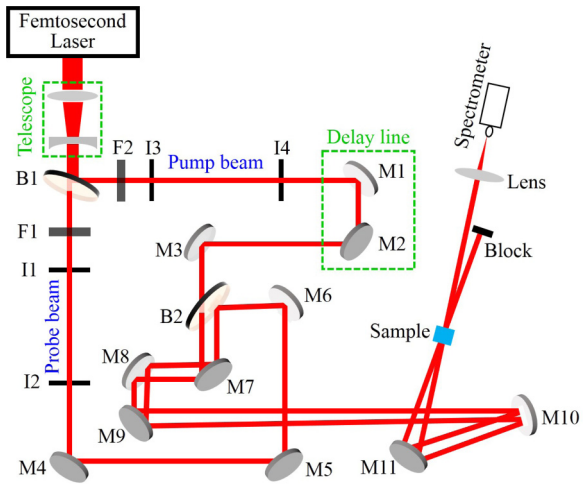

FIG. 3. The sketch of the experimental setup for the transient-absorption measurement. Here B1 and B2 are the fused silica beam splitters with the same thickness, F1 and F2 are the continuously variable neutral density (ND) filters with the same product model, I1–I4 are the irises, and M1–M11 are the high reflectively mirrors.

pulses. The probe and pump beams converge again on the beam splitter B2 with a small distance, and then propagate further to interact with the sample. Finally, the pump beam is blocked, and the probe beam is detected by a spectrometer (Ocean Optics, USB4000+).

The mirror M3 and beam splitter B2 are applied to adjust the spatial overlap of the pump and probe beams. The irises I2 and I4 are used to correct beam size of the probe and pump pulses, ensuring that the beam size of the pump pulse is larger than that of the probe pulse. The temporal overlap is tuned by the delay line according to the interference patterns of both beams. Both the temporal and spatial overlap of the probe and pump pulses at the interaction area are checked by a CCD camera, which can also be used to measure the beam size of the pump and probe pulses. The laser intensity is calculated by the measurable pulse duration, pulse energy, and beam size with a relative error of 4.8%. During the measurement, the probe-pulse intensity is fixed to be $I_{pr} = 5.6 \times 10^9$ W/cm^2, while the pump-pulse intensity I_{pu} is tuned from 1.2×10^{10} to 9.0×10^{10} W/cm^2, with a space of 6.0×10^9 W/cm^2. The 0.125 mM solution of the dye molecule IR144 in methanol carried by a spectrum cuvette (Ocean Optics, CSV500) with a path length of 0.5 mm is used as the sample, which is prepared in advance and kept in cold storage. The solution has enough time to reach solubility equilibrium, and the solvent effects can be eliminated. One absorption spectrum is averaged over 5×10^2 pulses. The nonlinear effects induced by the cuvette window can be ignored, which are checked by measuring the absorption spectra with an empty cuvette. From the configuration of the setup, we can find that both the probe and pump beams pass through the same ND filter and beam splitter, and the relative dispersion between the pump and probe pulse can be neglected.

IV. RESULTS AND DISCUSSIONS

Results in Figs. 4(a) and 4(b) show the measured time-delay-dependent absorption spectra of the dye molecules IR144 in liquid phase when the pump-pulse intensities are 1.2×10^{10} and 6.6×10^{10} W/cm^2, respectively. With a low pump-pulse intensity, the absorption spectrum does not exhibit any obvious changes when the time delay scans from negative to positive. This can be confirmed by the absorption spectra measured when the time delays are $\tau = \pm 20$ fs, as lined out in Fig. 4(a). They are similar no matter which laser pulse comes first to interact with the sample at this pump-pulse intensity. It means the system evolves freely after the excitation, i.e., the second arrival pulse or the first arrival pulse itself does not affect the molecular system excited by the first arrival pulse. When the pump-pulse intensity is tuned to be 6.6×10^{10} W/cm^2, the absorption spectra exhibit a time-delay dependence and an absorption minimum appears around 1.578 eV at $\tau = -50$ fs. When the time delay scans from -50 to 0 fs, the absorption minimum becomes more and more obvious and its position shifts to the low energy side. The absorption spectrum at $\tau = -20$ fs is lined out in Fig. 4(b) and shown by the blue solid line, from which one can find that the absorption spectrum is a wavy line with an absorption minimum at 1.570 eV and a maximum at 1.550 eV. However, the absorption spectrum changes differently when

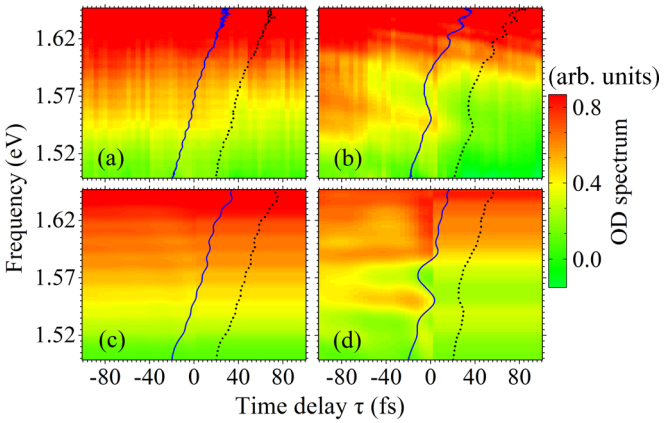

FIG. 4. The time-delay-dependent absorption spectra with a fixed probe-pulse intensity of $I_{pr} = 5.6 \times 10^9$ W/cm^2. (a) and (b) The experimental results with $I_{pu} = 1.2 \times 10^{10}$ W/cm^2 and $I_{pu} = 6.6 \times 10^{10}$ W/cm^2, respectively, while (c) and (d) display the corresponding simulation results. The absorption spectra at $\tau = -20$ fs and $\tau = 20$ fs are lined out in all these panels by the blue solid and black dotted lines, respectively. With $I_{pu} = 1.2 \times 10^{10}$ W/cm^2, the extracted phase changes $\{\phi^{B}_{N,i}\}$ are $\{0.096\pi, 0.096\pi, 0.093\pi, 0.089\pi, 0.092\pi, 0.091\pi, 0.084\pi, 0.095\pi, 0.094\pi, 0.089\pi\}$ for these ten electronic transition dipoles ranging from 1.527 to 1.644 eV, and $\{\phi^{B}_{P,i}\}$ are $\{-0.095\pi, -0.093\pi, -0.095\pi, -0.094\pi, -0.094\pi, -0.096\pi, -0.092\pi, -0.093\pi, -0.005\pi, -0.006\pi\}$. $\{\phi^{B}_{N,i}\}$ are $\{0.48\pi, 1.25\pi, 0.29\pi, 0.84\pi, 1.32\pi, 0.35\pi, 0.24\pi, 0.34\pi, 0.36\pi, 0.31\pi\}$, and $\{\phi^{B}_{P,i}\}$ are $\{-0.30\pi, -0.32\pi, -0.81\pi, -0.62\pi, -0.55\pi, -0.38\pi, -0.29\pi, -0.34\pi, -0.43\pi, -1.34\pi\}$, when the pump-pulse intensity is increased to $I_{pu} = 6.6 \times 10^{10}$ W/cm^2. The phase changes $\{\phi^{B}_{P,i}\}$ are shown with a subtraction of 2π to compare with the results on the probe-pump side.

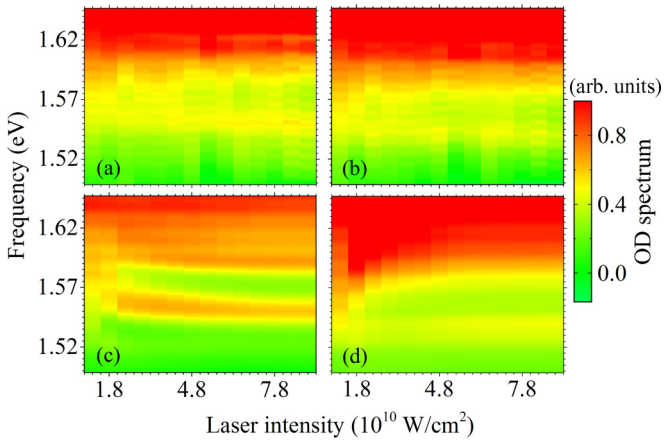

FIG. 5. The pump-pulse intensity-dependent absorption spectra. (a) and (b) The experimental results with time delays of $\tau = -20$ fs and $\tau = 20$ fs, respectively, while (c) and (d) display the corresponding simulation results. The probe-pulse intensity is fixed to $I_{pr} = 5.6 \times 10^9$ W/cm^2, while the pump-pulse intensity I_{pu} is tuned from 1.2×10^{10} to 9.0×10^{10} W/cm^2.

the time delay is tuned to be positive. For comparison, the wavy absorption spectrum at $\tau = 20$ fs is also lined out by the black dotted line, and both its minimum (1.560 eV) and maximum (1.542 eV) appear at different positions, indicating the different dynamics on the pump-probe and probe-pump sides.

With a pump intensity in the range of 10^{10} W/cm^2, the physics is slightly beyond third-order perturbation treatment, but it is far below the threshold of dissociation or ionization. The spectroscopy with such strong fields acts as a bridge between low-order perturbation and strong field regimes, and it will complicate the spectral features and the related analysis [19]. Higher order processes needed to be considered. These effects can be included in our theoretical frame by the phase modification factors, as demonstrated in the atomic system [27,40,41]. By artificially including phase changes to these ten electronic dipoles, the experimental results corresponding to these two different pump-pulse intensities are reproduced by the simulation, and results are displayed in Figs. 4(c) and 4(d). When the pump-pulse intensity is $I_{pu} = 1.2 \times 10^{10}$ W/cm^2, the pump pulse is too weak to induce significant modification to the system's dynamics no matter which pulse comes first, and no obvious change is found in the absorption spectral shape. The molecular phase changes $\phi^{B}_{N,i}$ for the probe-pump side and $\phi^{B}_{P,i}$ for the pump-probe side are almost zero, which are used to model the modulation and can be found in the caption of Fig. 4.

When the pump-pulse intensity is increased to be $I_{pu} = 6.6 \times 10^{10}$ W/cm^2, apparent changes are obtained in the absorption spectra, which indicates a modulation of the system's dynamic induced by the pump pulse. On the probe-pump side ($\tau < 0$), the probe pulse will first interact with the target molecule to excite the multilevel system, and the pump pulse comes to interact with the excited system a time $|\tau|$ later. This can be understood as quantum phase modulation first demonstrated in He [25]. The pump pulse will induce a transient energy shift of the excited states due to the Stark effect, and consequently phase changes of the electronic dipoles. The phase change is determined by the laser intensity as Eq. (5). With phase changes of $\phi^{B}_{N,i}$, the spectral response of each electronic dipole are modulated, resulting in the appearance of the absorption minimum. Although the phase changes are constant for a fixed pump-pulse intensity, the spectral shape changes with the time delay τ. It is caused by the different time when the phase changes happen to these dipoles. However, the electronic dipoles are modified differently on the pump-probe side ($\tau > 0$). The pump pulse both excites and modifies the phase of the molecular system. The second arrival probe pulse only plays the role to probe the system's dynamic evolution. In the simulation, the phase changes happen right after the excitation, which is different with that when $\tau < 0$. The phase changes $\phi^{B}_{P,i}$ are also extracted and shown with a subtraction of 2π in the caption of Fig. 4. The wavy absorption spectra at $\tau = \pm 20$ fs are lined out in Fig. 4(d), confirming that simulation agrees well with the experimental results.

Finally, we test the effect of the pump-pulse intensity on the changes in the molecular phase. Figures 5(a) and 5(b) show the absorption spectra measured at $\tau = -20$ fs and $\tau = 20$ fs with the pump-pulse intensity varying from 1.2×10^{10} to 9.0×10^{10} W/cm^2, respectively, while Figs. 5(c) and 5(d) are the simulation results. The absorption spectral shape changes with the pump-pulse intensity. With the increase of

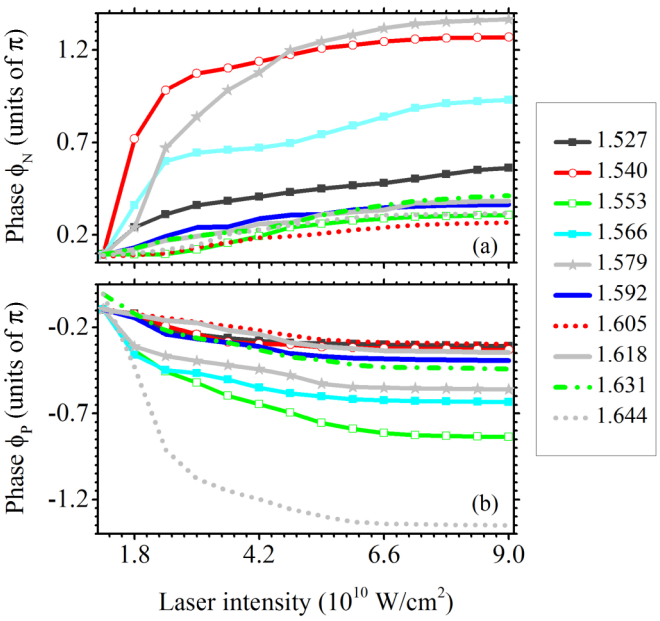

FIG. 6. The pump-pulse intensity-dependent phase evolution of the molecular system obtained by the artificial-phase method, when the probe pulse (a) precedes and (b) follows the pump pulse, respectively.

the pump-pulse intensity, an absorption minimum at 1.570 eV gradually emerges on the probe-pump side, inducing the split of the spectrum, i.e., another absorption maximum appears. The maximum shifts to lower energy with the increase of the pump-pulse intensity. However, its position is different for the same pump-pulse intensity on the pump-probe side, reflecting the different physical mechanisms acting at both sides.

The intensity-dependent spectral shape enables one to quantify the changes in the molecular phase ensuing from the interaction with strong pump pulses of varying intensity, as captured by $\phi^{\mathrm{B}}_{\mathrm{N},i}$ in Fig. 6(a) and $\phi^{\mathrm{B}}_{\mathrm{P},i}$ in Fig. 6(b). On the probe-pump side, the pump pulse strongly modifies the excited system generated by the probe pulse. The modulation effect increases with the pump-pulse intensity, showing as the increase of the phase changes of these different electronic dipoles $\phi^{\mathrm{B}}_{\mathrm{N},i}$. The pump pulse is responsible for the excitation of the system and the generation of initial phase changes on the pump-probe side. Results in Fig. 6(b) show these phases $\phi^{\mathrm{B}}_{\mathrm{P},i}$ reduce with the increase of pump-pulse intensity, whose tendencies are inverse with that of $\phi^{\mathrm{B}}_{\mathrm{N},i}$. We believe that it is the correlation between the excitation of the system and the generation of initial phase changes results in these different behaviors of the phase changes on the pump-probe side. These phase changes caused by the pump pulse reach saturation on both sides, which means the dipoles become more and more insensitive to the pump pulse with the increase of the pump-pulse intensity. Meanwhile, it can be found that the phase changes of these dipoles with low transition frequencies ($<$1.592 eV) are more sensitive to the pump pulse than that with high transition frequencies ($\geqslant$1.592 eV), no matter which pulse comes first, except for the dipole with a transition frequency 1.644 eV on the pump-probe side. It is known that the resonance and near-resonance effects may modulate a quantum system, showing as the change of the absorption spectrum. For our case, both effects are included in the phase modulation of the electronic dipoles and contribute to their phase changes. The laser pulse used in measurement has a central frequency of 1.569 eV and its spectrum mainly covers these transitions with low frequencies, i.e., the laser intensity at these frequencies is higher. For an electronic dipole, the resonance and near-resonance effects increase with the laser intensity at the transition frequency. That is why the phase changes of these dipoles with low transition frequencies are more sensitive to the pump pulse. Compared with the result in Ref. [37], it can be found that the laser bandwidth may affect the modulation induced by the pump pulse. The dependencies of these phase changes on the laser bandwidth and the central frequency of the pump pulse are needed to be further studied for the full understanding of the modulation effect.

V. CONCLUSIONS

In conclusion, we investigate the transient-absorption spectra of a complex molecular system to figure out how the molecular phases are encoded in the absorption spectra of the probe pulse on both the probe-pump and pump-probe sides. Strong laser fields are applied to modulate the phase evolution of the excited states after their excitation and thereby reconstruct the phase of the excited molecular system. The intensity-dependent phase information can be extracted from the dependence of the absorption spectra on the pump-pulse intensity, allowing us to quantify the dynamic evolution of the molecular system in intense laser fields. The presented strong-field modulation mechanism used in complex molecules in liquid phase goes beyond previous weak-field experimental approaches. This work not only marks an important step towards full reconstruction of complex molecular wave packets under intense laser field by relating the dynamic evolution of complex molecular systems to the absorption spectral shape, but also find us a way to understand the physics in the regime between low-order perturbation and strong field.

ACKNOWLEDGMENTS

The authors thank National Natural Science Foundation of China (Grants No. 11504148 and No. 11575073) and the Fundamental Research Funds for the Central Universities (Grant No. lzujbky-2016-35)

[1] G. Mackinney, J. Biol. Chem. **140**, 315 (1941).
[2] J. Petrich, J. Breton, J. Martin, and A. Antonetti, Chem. Phys. Lett. **137**, 369 (1987).
[3] W. T. Pollard and R. A. Mathies, Annu. Rev. Phys. Chem. **43**, 497 (1992).
[4] M. Holler, F. Schapper, L. Gallmann, and U. Keller, Phys. Rev. Lett. **106**, 123601 (2011).
[5] M. Wu, S. Chen, S. Camp, K. J. Schafer, and M. B. Gaarde, J. Phys. B **49**, 062003 (2016).

[6] C. Brif, R. Chakrabarti, and H. Rabitz, New J. Phys. **12**, 075008 (2010).

[7] F. Martín, Y. Cheng, M. Chini, X. Wang, A. González-Castrillo, A. Palacios, L. Argenti, and Z. Chang, J. Phys.: Conf. Ser. **635**, 112070 (2015).

[8] E. Goulielmakis, Z.-H. Loh, A. Wirth, R. Santra, N. Rohringer, V. S. Yakovlev, S. Zherebtsov, T. Pfeifer, A. M. Azzeer, M. F. Kling, S. R. Leone, and F. Krausz, Nature (London) **466**, 739 (2010).

[9] L. J. Zipp, A. Natan, and P. H. Bucksbaum, Optica **1**, 361 (2014).

[10] H. Wang, M. Chini, S. Chen, C.-H. Zhang, F. He, Y. Cheng, Y. Wu, U. Thumm, and Z. Chang, Phys. Rev. Lett. **105**, 143002 (2010).

[11] S. Chen, M. Wu, M. B. Gaarde, and K. J. Schafer, Phys. Rev. A **88**, 033409 (2013).

[12] C.-T. Liao, A. Sandhu, S. Camp, K. J. Schafer, and M. B. Gaarde, Phys. Rev. Lett. **114**, 143002 (2015).

[13] W. Zhang, C.-C. Shu, T.-S. Ho, H. Rabitz, and S.-L. Cong, J Chem. Phys. **140**, 094304 (2014).

[14] M. F. Ciappina, J. A. Pérez-Hernández, A. S. Landsman, W. A. Okell, S. Zherebtsov, B. Förg, J. Schötz, L. Seiffert, T. Fennel, T. Shaaran, T. Zimmermann, A. Chacón, R. Guichard, A. Zaïr, J. W. G. Tisch, J. P. Marangos, T. Witting, A. Braun, S. A. Maier, L. Roso, M. Krüger, P. Hommelhoff, M. F. Kling, F. Krausz, and M. Lewenstein, Rep. Prog. Phys. **80**, 054401 (2017).

[15] L. Seiffert, Q. Liu, S. Zherebtsov, A. Trabattoni, P. Rupp, M. C. Castrovilli, M. Galli, F. Süßmann, K. Wintersperger, J. Stierle, G. Sansone, L. Poletto, F. Frassetto, I. Halfpap, V. Mondes, C. Graf, E. Rühl, F. Krausz, M. Nisoli, T. Fennel, F. Calegari, and M. F. Kling, Nat. Phys. **13**, 766 (2017).

[16] A. Monmayrant, B. Chatel, and B. Girard, Phys. Rev. Lett. **96**, 103002 (2006).

[17] Z.-H. Loh, M. Khalil, R. E. Correa, R. Santra, C. Buth, and S. R. Leone, Phys. Rev. Lett. **98**, 143601 (2007).

[18] A. R. Attar, A. Bhattacherjee, and S. R. Leone, J. Phys. Chem. Lett. **6**, 5072 (2015).

[19] H. Shen, Y. Zhang, T.-M. Yan, Z. Wang, and Y. Jiang, Chem. Phys. **476**, 17 (2016).

[20] Y. Cheng, M. Chini, X. Wang, A. González-Castrillo, A. Palacios, L. Argenti, F. Martín, and Z. Chang, Phys. Rev. A **94**, 023403 (2016).

[21] J. E. Bækhøj, L. Yue, and L. B. Madsen, Phys. Rev. A **91**, 043408 (2015).

[22] P. Lan, M. Ruhmann, L. He, C. Zhai, F. Wang, X. Zhu, Q. Zhang, Y. Zhou, M. Li, M. Lein, and P. X. Lu, Phys. Rev. Lett. **119**, 033201 (2017).

[23] M. Schultze, K. Ramasesha, C. Pemmaraju, S. Sato, D. Whitmore, A. Gandman, J. S. Prell, L. J. Borja, D. Prendergast, K. Yabana, D. M. Neumark, and S. R. Leone, Science **346**, 1348 (2014).

[24] V. Kuntermann, C. Cimpean, G. Brehm, G. Sauer, C. Kryschi, and H. Wiggers, Phys. Rev. B **77**, 115343 (2008).

[25] C. Ott, A. Kaldun, P. Raith, K. Meyer, M. Laux, J. Evers, C. H. Keitel, C. H. Greene, and T. Pfeifer, Science **340**, 716 (2013).

[26] A. Kaldun, A. Blättermann, V. Stooß, S. Donsa, H. Wei, R. Pazourek, S. Nagele, C. Ott, C. D. Lin, J. Burgdörfer, and T. Pfeifer, Science **354**, 738 (2016).

[27] Z. Liu, Q. Wang, J. Ding, S. M. Cavaletto, T. Pfeifer, and B. Hu, Sci. Rep. **7**, 39993 (2017).

[28] H. Hasegawa and Y. Ohshima, Phys. Rev. Lett. **101**, 053002 (2008).

[29] S. L. Johnson, E. Vorobeva, P. Beaud, C. J. Milne, and G. Ingold, Phys. Rev. Lett. **103**, 205501 (2009).

[30] C. Ott, A. Kaldun, L. Argenti, P. Raith, K. Meyer, M. Laux, Y. Zhang, A. Blättermann, S. Hagstotz, T. Ding, R. Heck, J. Madroñero, F. Martin, and T. Pfeifer, Nature (London) **516**, 374 (2014).

[31] S. M. Cavaletto, Z. Harman, T. Pfeifer, and C. H. Keitel, Phys. Rev. A **95**, 043413 (2017).

[32] A. H. Zewail, J. Phys. Chem. A **104**, 5660 (2000).

[33] R. Leonhardt, W. Holzapfel, W. Zinth, and W. Kaiser, Chem. Phys. Lett. **133**, 373 (1987).

[34] A. Stolow and J. G. Underwood, Time resolved photoelectron spectroscopy of nonadiabatic dynamics in polyatomic molecules, in *Advances in Chemical Physics* (Wiley-Blackwell, London, 2008), Chap. 6, pp. 497–584.

[35] T. Brixner, J. Stenger, H. M. Vaswani, M. Cho, R. E. Blankenship, and G. R. Fleming, Nature (London) **434**, 625 (2005).

[36] G. Panitchayangkoon, D. Hayes, K. A. Fransted, J. R. Caram, E. Harel, J. Wen, R. E. Blankenship, and G. S. Engel, Proc. Natl. Acad. Sci. USA **107**, 12766 (2010).

[37] K. Meyer, Z. Liu, N. Müller, J.-M. Mewes, A. Dreuw, T. Buckup, M. Motzkus, and T. Pfeifer, Proc. Natl. Acad. Sci. USA **112**, 15613 (2015).

[38] K. Meyer, Ph.D. thesis, Max-Planck Institute for Nuclear Physics, 2014.

[39] J.-M. Mewes, Z.-Q. You, M. Wormit, T. Kriesche, J. M. Herbert, and A. Dreuw, J. Phys. Chem. A **119**, 5446 (2015).

[40] Z. Liu, S. M. Cavaletto, C. Ott, K. Meyer, Y. Mi, Z. Harman, C. H. Keitel, and T. Pfeifer, Phys. Rev. Lett. **115**, 033003 (2015).

[41] A. Blättermann, C. Ott, A. Kaldun, T. Ding, and T. Pfeifer, J. Phys. B **47**, 124008 (2014).

[42] U. Fano and J. W. Cooper, Rev. Mod. Phys. **40**, 441 (1968).

[43] X. Zhang, B. Li, and C. Gao, Appl. Phys. Lett. **89**, 112120 (2006).